NAL Proposal # 523
Spokesman: A. R. Dzierba
Dept. of Physics
Indiana University
Bloomington, Ind.
FTS: 331-6883

A Proposal To Study Multiparticle Peripheral Hadron Reactions Yielding Forward π^0 and η^0 Mesons

Abstract

We plan to make a systematic study of multiparticle peripheral hadron reactions yielding forward-going π^0 and η^0 mesons. We plan to carry out these studies at several energies between 20 and 200 GeV/c. The proposal is to study these reactions by installing the CIT photon detector (used in the $\pi^- p$ charge exchange experiment, E111) in the multiparticle spectrometer (currently being used for E110/E260). The physics goals include a search for new particle states in the $\pi^+\pi^-\pi^0$, $\pi^+\pi^-\eta^0$, $K^0\pi^0$, $K^0K^0\pi^0$ mass spectra up to large effective masses, a study of the dynamics (s and t dependences) of the production of known particles (ω^0, η', etc.) and a study of forward Δ^+ and N^{*+} in π-induced reactions. The detection efficiencies and effective mass resolutions for these final states are quite good. We will collect data on these reactions by running in a multiple-trigger configuration.

A. Barnes, G. Fox, R. Gomez, R. Kennett, J. Pine, and R. Walker
California Institute of Technology, Pasadena, California

B. Brabson, R. Crittenden, A. Dzierba, R. Heinz, and J. Krider
Indiana University, Bloomington, Indiana

Contents

		Page
I.	Physics Motivation	1
	A. Introduction	1
	B. Production Dynamics of Known Resonances	2
	C. Meson Spectroscopy	6
	D. Spectroscopy of Unknown Resonances	8
	E. Other Processes Involving Peripheral Production of Meson Resonances	9
	F. Baryon Exchange Processes	9
II.	The Multiparticle Spectrometer	11
III.	Characteristics of the Photon Detector	15
IV.	Acceptance and Yield Calculation	20
	Summary	33
	References	34

I. Physics Motivation

A. Introduction

This is a proposal to study multiparticle peripheral reactions yielding a forward-going π^o. The general class of reactions to be studied are described by the process

$$A + p \rightarrow C + D \qquad (1)$$

where

A - is an incident π, K, p or $\bar{p}$;

C - is a peripherally-produced (forward in the lab) resonance or a system of particles which decays into one, two, or three particles and a π^o (e.g., $C = \omega^o \rightarrow \pi^+\pi^-\pi^o$); and

D - is a one, two, or three particle system produced with low momentum in the lab.

The study of reaction (1) when C and D are stable particles or resonances is particularly interesting from a theoretical point of view in that we can test the various models which make predictions about the dynamics (s and t dependences) of the two-body process. An an example, the charge exchange reaction

$$\pi^- p \rightarrow \pi^o n \qquad (2)$$

is described remarkably well by a simple Regge-pole model in which the ρ trajectory is exchanged. The model describes the data over the energy range extending from 20 to 200 GeV.[1] The question as to whether other reactions can be understood in terms of simple Regge exchanges is theoretically relevant. The study of reaction (1) is also of interest at high energies in that we can examine the effective mass of a system of particles containing

a π^o to search for new resonances or study those resonances which are presently ambiguous. In fact, as we shall see below, the $\pi^+\pi^-\pi^o$ system is particularly rich in resonances which are both well established (e.g., again $\omega^o \to \pi^+\pi^-\pi^o$) and ambiguous (e.g., $A_1 \to \pi^+\pi^-\pi^o$).

A subset of reactions which are of the type described by (1) is currently under study by members of Fermilab experiment E110 using the Multiparticle Spectrometer (MPS) in the M6 beamline. In that experiment the forward going system, C, is required to decay into charged particles or into a K_s^o or Λ^o which are observed in their charged particle decay modes. Thus while that experiment studies a broad class of reactions the scope of the study of (1) is greatly enhanced by including those processes in which a forward π^o is produced. We discuss this point in detail below.

We propose to carry out this experiment by using the MPS facility currently being completed and used by members of the E110-260 collaboration.[2,3] To this spectrometer we will add the CIT photon detector (hereafter referred to as the photon detector) used in the π^-p charge-exchange experiment (Fermilab experiment E111).[4] A brief discussion of the characteristics of the MPS and the photon-detector are given in Sections II and III, respectively. To satisfy the impatient reader unwilling to wait for further details later, this combination of MPS and photon detector provides momentum measurement and particle identification of the forward going charged particles and a position and energy measurement of the forward going π^o.

B. Production Dynamics of Known Meson Resonances

Consider the reaction

$$\begin{array}{l} \pi^- p \to C\ n \\ \qquad\quad \hookrightarrow \pi^+\pi^-\pi^o \\ \qquad\qquad\qquad \hookrightarrow \gamma\gamma \end{array} \qquad (3)$$

which is one of the reactions we plan to study and is particularly rich in physics interest as we shall see. [In this proposal our discussion will focus on π^- induced reactions. We do plan to also study corresponding reactions with incident π^+, K^-, K^+, p and $\bar{p}$ which will have somewhat similar trigger topologies.]

The first important feature of reaction (3) is that system C has net neutral charge. Thus, if we view the production of C in some sort of exchange picture

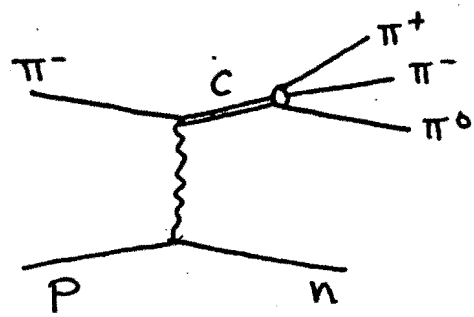

we see that Pomeron exchange(or to put it another way, diffraction dissociation) is ruled out. Thus, the $\pi^+\pi^-\pi^o$ is an attractive channel to search for G = -1 resonances produced with low cross sections since this channel, being neutral, is free from diffractive backgrounds which have relatively high cross sections which change slowly with energy.

The simple topology of reaction (3) readily lends itself to a simple trigger requirement which is two charged particles forward, two photons from the π^o in the photon detector, and no slow-charged particles or π^o's produced nearly at rest. We shall consider production of resonances which decay into a $\pi^+\pi^-\pi^o$. For ready reference we list the meson resonances with this decay mode in Table I. Since the photon detector can also detect the decay η^o through its 2γ decay mode, we also include those resonances which decay into $\pi^+\pi^-\eta^o$ and will be produced in

Table I. Meson Resonances Which Decay Into $\pi^+\pi^-\pi^o$ or $\pi^+\pi^-\eta^o$ [a]

Resonance	J^P	I^G	Partial Decay Mode	Fraction [b]
$\eta(548)$	0^-	0^+	$\pi^+\pi^-\pi^o$	24%
$\omega^o(783)$	1^-	0^-	$\pi^+\pi^-\pi^o$	90%
$\eta'(958)$	0^-	0^+	$\pi^+\pi^-\eta^o$	17%
			$\rho^o\gamma \to (\pi^+\pi^-)\gamma$	30%
$\phi(1020)$	1^-	0^-	$\pi^+\pi^-\pi^o$	16%
$A_1^o(1100)$	1^+	1^-	$\rho^\pm\pi^\mp \to (\pi^\pm\pi^o)\pi^\mp$	100%
$B^o(1235)$	1^+	1^+	$\omega^o\pi^o \to (\pi^+\pi^-\pi^o)\pi^o$	90% [c]
$D(1285)$	?	0^+	$\pi^+\pi^-\eta^o$	38%
$A_2^o(1310)$	2^+	1^-	$\rho^\pm\pi^\mp \to (\pi^\pm\pi^o)\pi^\mp$	23%
			$\eta^o\pi^o \to (\pi^+\pi^-\pi^o)\pi^o$	4% [c]
			$\omega^o\pi^+\pi^- \to (\pi^o\gamma)\pi^+\pi^-$	1% [c,d]
$E(1420)$	?	0^+	$K^+K^-\pi^o$	13% [c]
			$\pi^+\pi^-\eta^o$	26%
$\rho'(1600)$	1^-	1^+	$\rho^+\rho^- \to (\pi^+\pi^o)(\pi^-\pi^o)$	? [c,e]
$A_3^o(1640)$	2^-	1^-	$f^o\pi^o \to (\pi^+\pi^-)\pi^o$	67%
$\omega(1675)$	3^-	0^-	$\pi^+\pi^-\pi^o$	100%
$K^*(890)$	1^-	½	$K_S^o\pi^o \to \pi^+\pi^-\pi^o$	10%
$Q^o(1200)$	?	½	$K^+\pi^-\pi^o$	? [c,f]
$L(1770)$	?	½	$K^+\pi^-\pi^o$	? [c,f]

[a] From "Reviews of Particle Properties", Rev. Mod. Phys. Vol. 48, No. 2, Part II, April, 1976.

[b] These fractions take into account measured branching fractions and isospin considerations into the final state listed. When an η^o is listed as the end product of a decay we assume it is observed through its 2γ decay which 38% of all η decays.

[c] Listed since the final state is +,- neutrals.

[d] $(\omega^o \to \pi^o\gamma)/(\omega^o \to \text{all}) = 9\%$ is assumed.

[e] $\rho' \to 4\pi$ is dominant

[f] $K\pi\pi$ dominant

$$\pi^- p \to C\ n \quad C \to \pi^+\pi^-\eta^0 \quad \eta^0 \to \gamma\gamma \tag{4}$$

1. η^0 Production

The reaction

$$\pi^- p \to \eta^0\ n \quad \eta^0 \to \pi^+\pi^-\pi^0 \tag{5}$$

has been studied by the E111 collaboration and has been described, in the Regge picture, by exchange of the A_2-pole.[1] Our interest in measuring (5) will mainly be to compare our data with that of E111.

2. ω^0 Production

Production of ω^0 can take place either via natural parity exchange (ρ-trajectory) or unnatural parity exchange (B-trajectory).

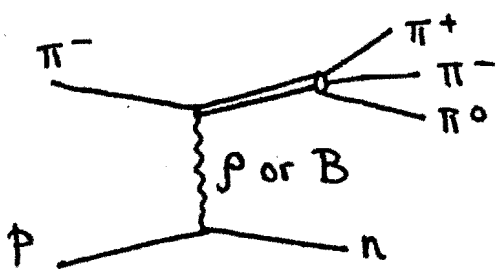

At lower energies (p_{LAB} = 3.7 to 5.5 GeV/c)[5] it appears that ρ- and B-exchange contributions are roughly comparable with some indication that the B-exchange contribution is falling faster with energy as one might expect. The density-matrix elements of the ω^0 measure the amount of ρ- and B-exchange.

3. η' Production

The reaction

$$\pi^- p \to \eta' n \tag{6}$$

will be measured with η' observed via its $\eta^0\pi^+\pi^-$ and $\rho^0\gamma$ decay modes (see Table I). The study of n and η' cross sections has seen recent theoretical interest because of the sensitivity to mixing ideas and theories as to why ϕ and not η' obeys "Zweig's rule".[6]

C. Meson Spectroscopy[7]

Though there has been a lot of attention of late paid to charm meson searches there are still gaps to be filled in the charmless $q\bar{q}$ (quark-antiquark) states predicted by the quark model. For completeness we list the L = 0 and L = 1 quark states:

Table II: L = 0 Quark States

$J^{PC} = 0^{-+}$	π, K, η, η'
$J^{PC} = 1^{--}$	ρ, K^*, ω, ϕ

Table III: L = 1 Quark States

J^P / isospin	0^+ Nonet	1^+ "B" Nonet	1^+ "A_1" Nonet	2^+ Nonet
I = 1	π_N(980)	B(1235)	A_1(1070)	A_2(1310)
Strange I = ½	κ ($\approx$ 1250)	Q_B(1300 → 1400)	Q_{A_1} = C(?) (1240 → 1290)	K_N^* (1420)
I = 0 singlet/octet mixing (?)	ε ($\approx$ 750)	h (?)	D (1285)	f^0(1260)
	S^*($\approx$ 1000)	h' (?)	D' = E(1422) ? or M(953) ?	f'(1514)

The decays and measured or predicted widths for the 0^+ and 1^+ mesons where many ofthe gaps exist are listed below in Table IV (source: Reference 7). We expect to be sensitive to many of these decay channels.

Table IV: 0^+, 1^+ Meson Decays

Particle	Mass GeV	Decay	Width MeV	Source of Width
π_N (980)	0.98	$\pi\eta$	40	(a)
B (1235)	1.235	$\pi\omega$	100	Expt
Q_B	1.380	$K\rho$ $K^*\pi$ $K\omega$	32 80 9	(b)
h(octet - ?)	1.01	$\pi\rho$	40	(b)
h(magic -ω - ?)	1.25	$\pi\rho$	330	(b)
h'(magic -ϕ)	1.5	$\bar{K}K^* + K\bar{K}^*$	75	(b)
A_1	1.07	$\pi\rho$	140	"Expt"
Q_{A_1} = C	1.24	πK^*	50	(c)
D (1285)	1.285	$\eta\pi\pi$ $K\bar{K}\pi$	$\Gamma_{tot} = 21 \pm 10$	Expt
D' (magic -ϕ) = E (?)	1.422	$\bar{K}K^* + K\bar{K}^*$	50	(c)
D' (singlet)	any	$\bar{K}K^* + K\bar{K}^*$	0	(c)

Sources: (a) SU_3 and $\varepsilon \to \pi\pi$ = 300 MeV
(b) SU_3 and $B \to \pi\omega$ = 100 MeV
(c) SU_3 and $A_1 \to \pi\rho$ = 140 MeV

D. Spectroscopy of Unknown Resonances

a. $\pi^+\pi^-\pi^o$ and $\pi^-\pi^-\eta^o$ channels

For the purpose of doing meson spectroscopy we would very likely study the $\pi^+\pi^-\pi^o$ or $\pi^+\pi^-\eta^o$ spectrum in the semi-inclusive mode, (i.e., without regard to the nature of the system of particles D in reaction (1). For example, there are two ρ' states, an unestablished one at 1250 MeV and an established one at 1600 MeV. There should be ω' states in the corresponding SU_3 multiplets. Thus, in the $\pi^+\pi^-\pi^o$ events we will be specifically looking in the 1200 MeV and 1600 MeV mass regions, where these ρ' $J^P = 1^-$ states could exist.

b. Charm Spectroscopy

This experiment will also be sensitive to charmed particles produced with $x \gtrsim 0.5$. The channel $K_s^o\pi^o$ will be studied simultaneously with the $\pi^+\pi^-\pi^o$ channel. The neutral Vee decay ($K_s^o \to \pi^+\pi^-$) topology will be used as a trigger requirement. This will allow us to search for charm mesons. For example, we will be sensitive to the decays

$$D^o \to \bar{K}^o\pi^o$$
$$\quad\quad \hookrightarrow \pi^+\pi^-$$

$$D^o \to K^o\pi^o\pi^o$$
$$\quad\quad \hookrightarrow \pi^+\pi^-$$

These channels are again attractive for doing charm search in that they are free of diffractive backgrounds. The expected $K^o\pi^o$ mass resolution (~10 MeV) should allow us to identify narrow resonances.

E. Other Processes Involving Peripheral Production of Meson Resonances

Examples of other physics which can be studied experimentally with forward-neutral detection are the reactions:

$$K^- p \to K^- \pi^o \quad p \qquad (7)$$
$$\quad\quad \hookrightarrow \gamma\gamma$$

$$K^- p \to K^- \omega^o \quad p \qquad (8)$$
$$\quad\quad \hookrightarrow \pi^+ \pi^- \pi^o$$
$$\quad\quad\quad\quad \hookrightarrow 2\gamma$$

From an experimental point-of-view, the single charged particle forward simplifies the particle identification problem. A comparison of the $K^-\pi^o$ vs. $K^-\omega^o$ is interesting from the point-of-view of exchange dynamics and spectroscopy since the $K^-\pi^o$ system can have I = 1/2 or 3/2 with J^P constrained to be 0^+, 1^-, 2^+, . . . while in the $K^-\omega^o$ system I = 1/2 with J^P no longer constrained to be in the natural spin-parity sequence.

F. Baryon Exchange Processes

Another example of a subset of reaction (1) is the peripheral production of Δ^+ and N^{*+} resonances in baryon exchange processes:

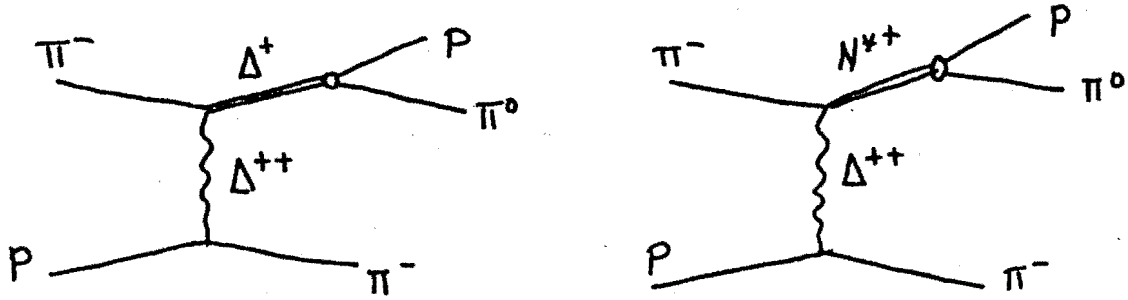

These processes are again interesting from a Regge picture since they proceed via exchange of a single Regge pole, the Δ^{++}. Again, the presence of a single charged particle forward eases the experimental task of

particle identification. In addition to the π^- induced reaction, we would also study

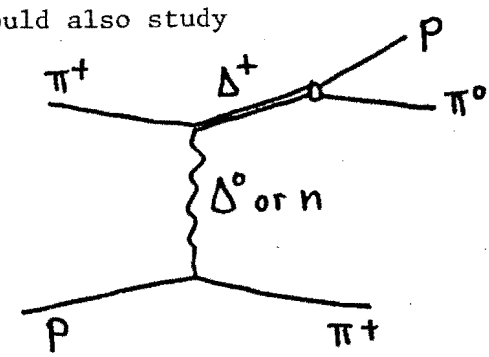

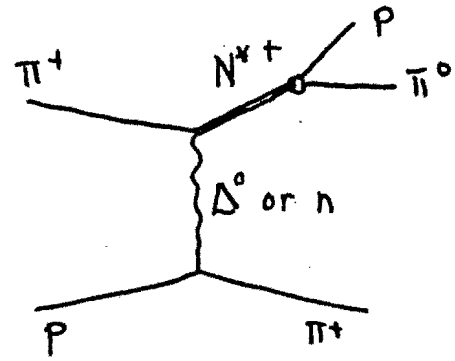

which proceed by Δ^o or n exchange. The comparison of these processes with the corresponding backward elastic scattering reactions would allow one to sort out dynamical effects arising from exchanges (which are the same) or the vertices (which are different). Does the dip in the backward π^+p elastic scattering persist at high energies, and is it present in both $\pi^+p \to \Delta^+\pi^+$ and $\pi^+p \to p\pi^+$? Is there peak shrinkage in $\pi^-p \to p\pi^-$ and $\pi^-p \to \Delta^+\pi^-$? We will also study the dynamics of forward N^* production and inclusive $(p\pi^o)$ forward systems.

The question of the proper dynamical framework in which to consider u-channel reactions at high energies is open. Instead of the above exchange picture, Feynman's hadronic Bremsstrahlung idea or a geometric model might be most appropriate. It is also possible that a parton picture might apply. Thus, we envision our proposed measurements of high energy $\pi^\pm p \to \Delta^+\pi^\pm$ scattering to be exploratory.

II. The Multiparticle Spectrometer (MPS)

A. Overall View

The MPS is described in References 2 and 3. An overall view of the spectrometer is shown in Figure 1. A more detailed view of the upstream end of the spectrometer is shown in Figure 2.

B. A Tour of the MPS

If the reader will refer to Figure 1 we will take a quick tour of the MPS starting at the upstream end.

1. Beam

The M6 beam line will deliver positive and negative particles from 20 GeV/c to 200 GeV/c. The beam line instrumentation currently includes 4 Cerenkov counters: two threshold counters, a differential counter, and a DISC counter.

2. Target Region (refer to Figure 2)

The target region includes, in addition to a 1 foot hydrogen target,

a. scintillation counters (S_A, S_B, S_C);

b. proportional wire chamber planes (1 mm spacing) just upstream and downstream of the target, (BB and A);

c. shower counters (lead-scintillator modules) V_o, V_2, and V_3 which will be used to detect the presence of slow π^o;

d. cylindrical shower counter (V_1) which is a lead scintillator array. The scintillator is segmented in strips parallel to the beam direction. These strips divide the azimuth into 24 segments which can be separately interrogated for presence of a slow π^o;

TOP VIEW - MULTIPARTICLE SPECTROMETER

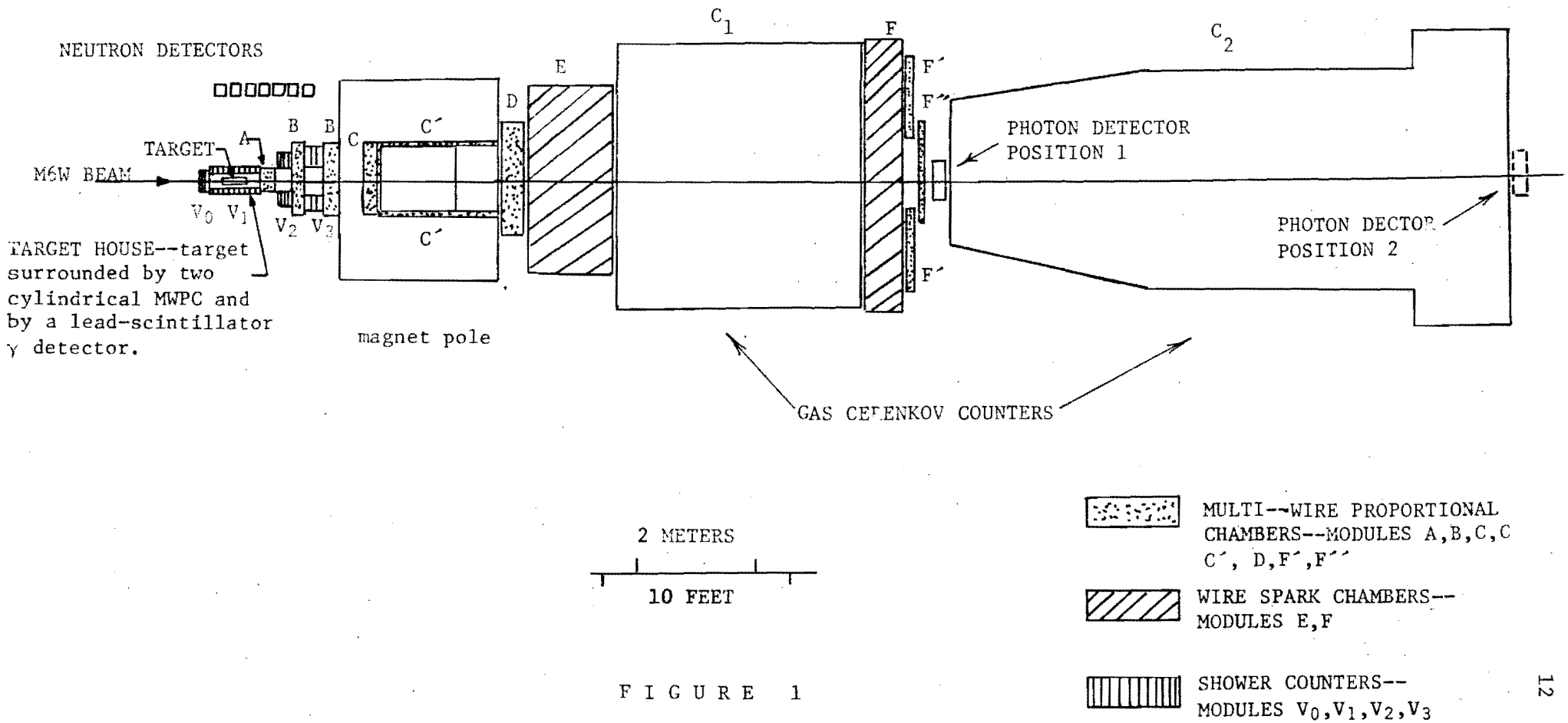

F I G U R E 1

UPSTREAM VIEW OF SPECTROMETER

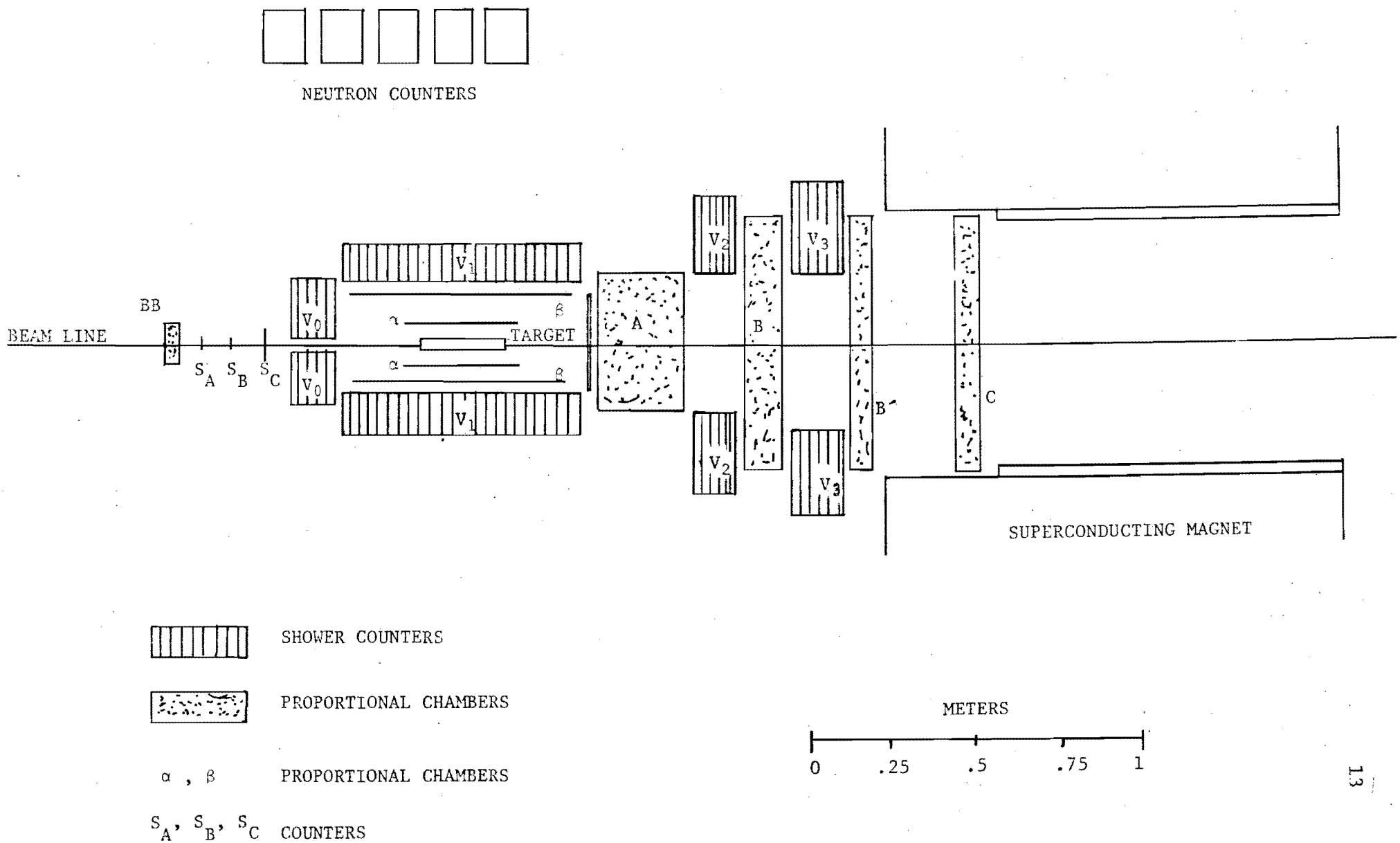

FIGURE 2

e. cylindrical proportional wire chambers (α,β) with wires parallel to the beam line. These wires divide the azimuth into 48 segments and can be used in the trigger for particle counting. The longitudinal coordinate will be read out by current-division electronics;

f. neutron counters;

g. a possible MWPC just downstream of VO. We are doing Monte Carlo studies to see if this is needed to improve the acceptance for the backward π in the baryon exchange reactions.

3. Proportional-wire planes at Stations B, C, C' (lining magnet walls), D, F', and F". These wires are available in the trigger for making multiplicity requirements.

4. Spark chambers at Stations E and F.

5. A 2 ft. x 4 ft. x 4 ft. superconducting magnet with a $\int B \cdot dl$ = 18 kg-m.

6. Atmospheric gas threshold Cerenkov counters C_1 and C_2 with segmented mirror planes (22 segments for C_1, 16 for C_2).

III. Characteristics of the Photon Detector[8]

A. Overview

The photon detector is a hodoscope shower detector which effectively samples the depth integrated transverse projection of electromagnetic showers in two orthogonal transverse dimensions. Figure 3 shows a schematic diagram of the detector. The plates are stacked normal to the direction of incident particles (z) with gaps between them of approximately 7 mm. These gaps are filled with long narrow scintillation fingers, 1.05 cm wide, which are close-packed and run the full width of the detector. Vertical and horizontal fingers are in successive gaps. The eight fingers having the same x coordinate or the same y coordinate are connected optically by curved light pipes at one end, and each set of eight fingers so connected constitutes one counter. There are 70 x-counters and 70 y-counters. Each finger has been wrapped with foil of graded reflectivity, and a light trap captures those transmitted at large angles to the finger axis. Because of this special treatment, each counter yields pulses of uniform height (within 2%) over the entire counter length.

B. Detector Resolution

The resolution of the photon detector for various processes can be calculated from the resolution for single photons. The energy resolution for single photons is understood in terms of two effects: the statistical fluctuations in the shower process and the spatial non-uniformity of the detector response. The statistical fluctuations dominate the resolution at low energies and can be represented by $\Delta E(\text{rms}) \simeq \pm .18\sqrt{E}$ (E and ΔE in GeV). At high energies the spatial non-uniformity limits the energy resolution to $\Delta E(\text{rms}) \simeq \pm .03\sqrt{E}$. The position resolution for single photons is $\Delta x(\text{rms}) \simeq \pm 1$ mm.

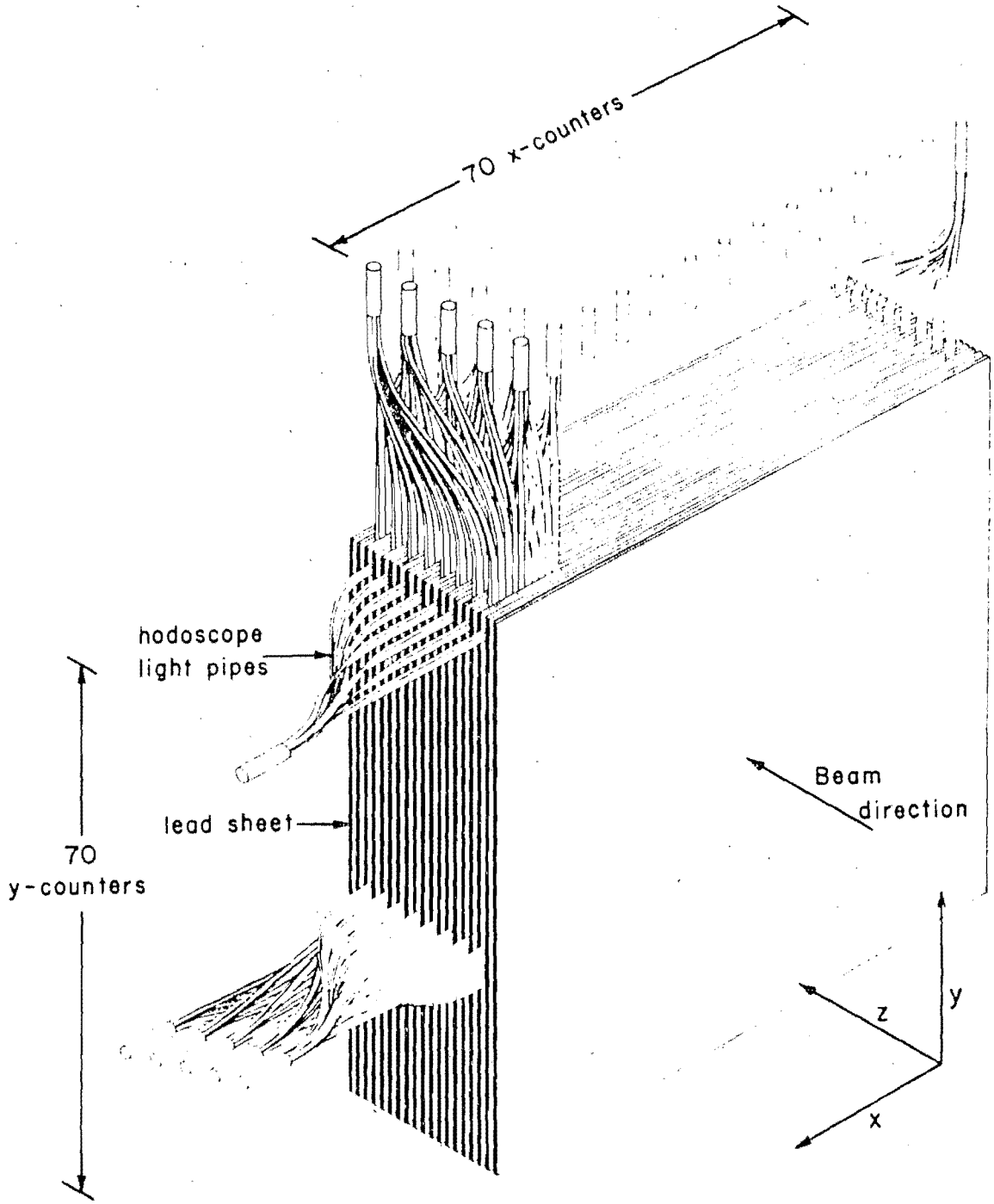

Figure 3: The Photon Detector

The resolution for multi photon states depends on the apparatus configuration and the details of the decay kinematics. A π^0 position resolution of $\Delta x(\text{rms}) \simeq \pm 2$ mm is representative. Typical msss spectra from data taken during E111 ($\pi^- p$ charge exchange) are shown in Figures 4 and 5.

C. Interface

Currently the photon-detector is interfaced to its host computer (a Sigma 2). In addition to the Sigma 2 software used to read in and analyze the data there is software to continually calibrate the detector during interspill time. We envisage keeping the Sigma 2 photon-detector link intact and will interface the Sigma 2 to the MPS online PDP11 computer.

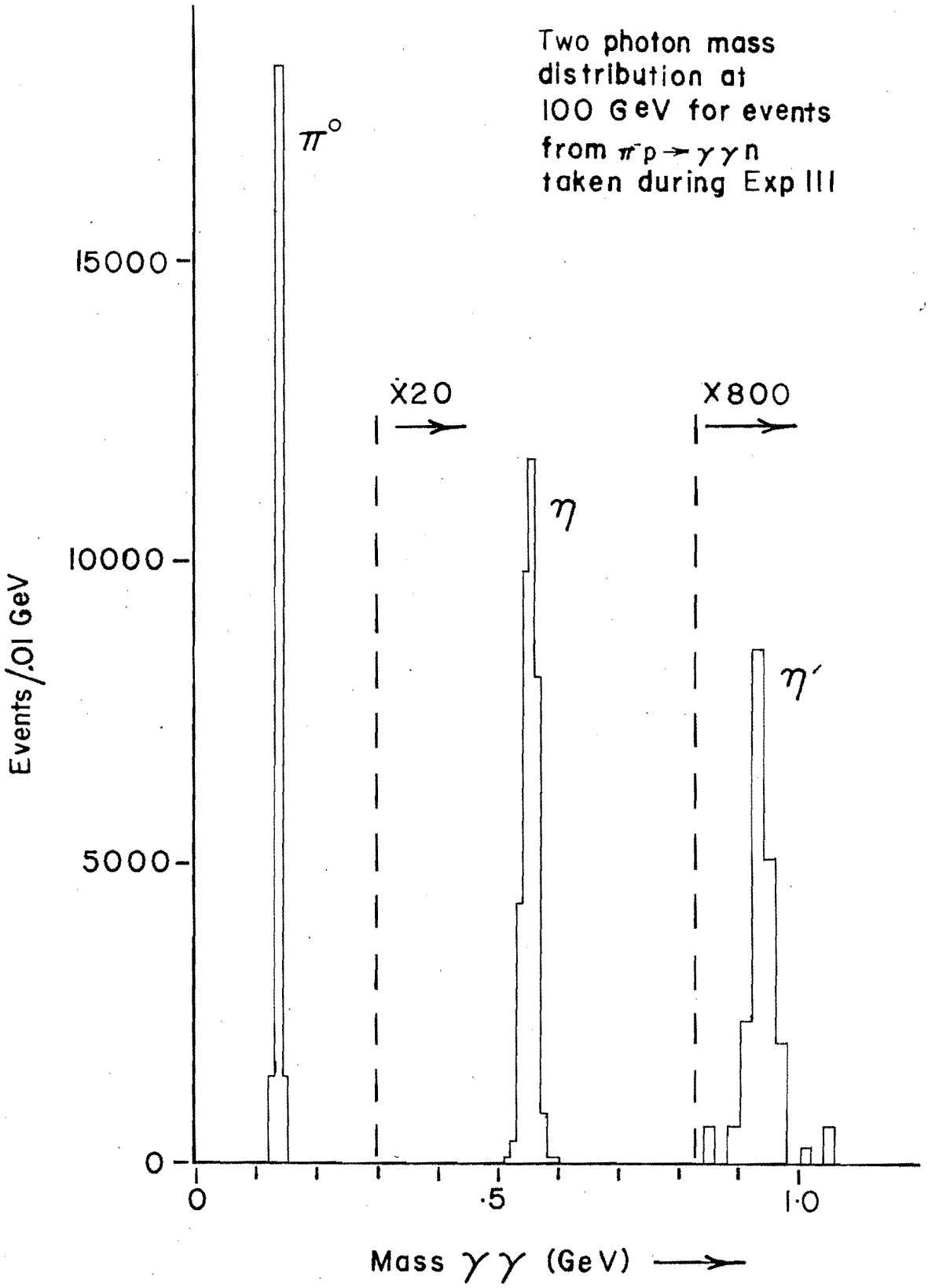
Two photon mass distribution at 100 GeV for events from $\pi^- p \to \gamma\gamma n$ taken during Exp III
π^0
η
η'
X20
X800
15000
10000
5000
0
Events /.01 GeV
0
.5
1.0
Mass $\gamma\gamma$ (GeV)

FIGURE 4

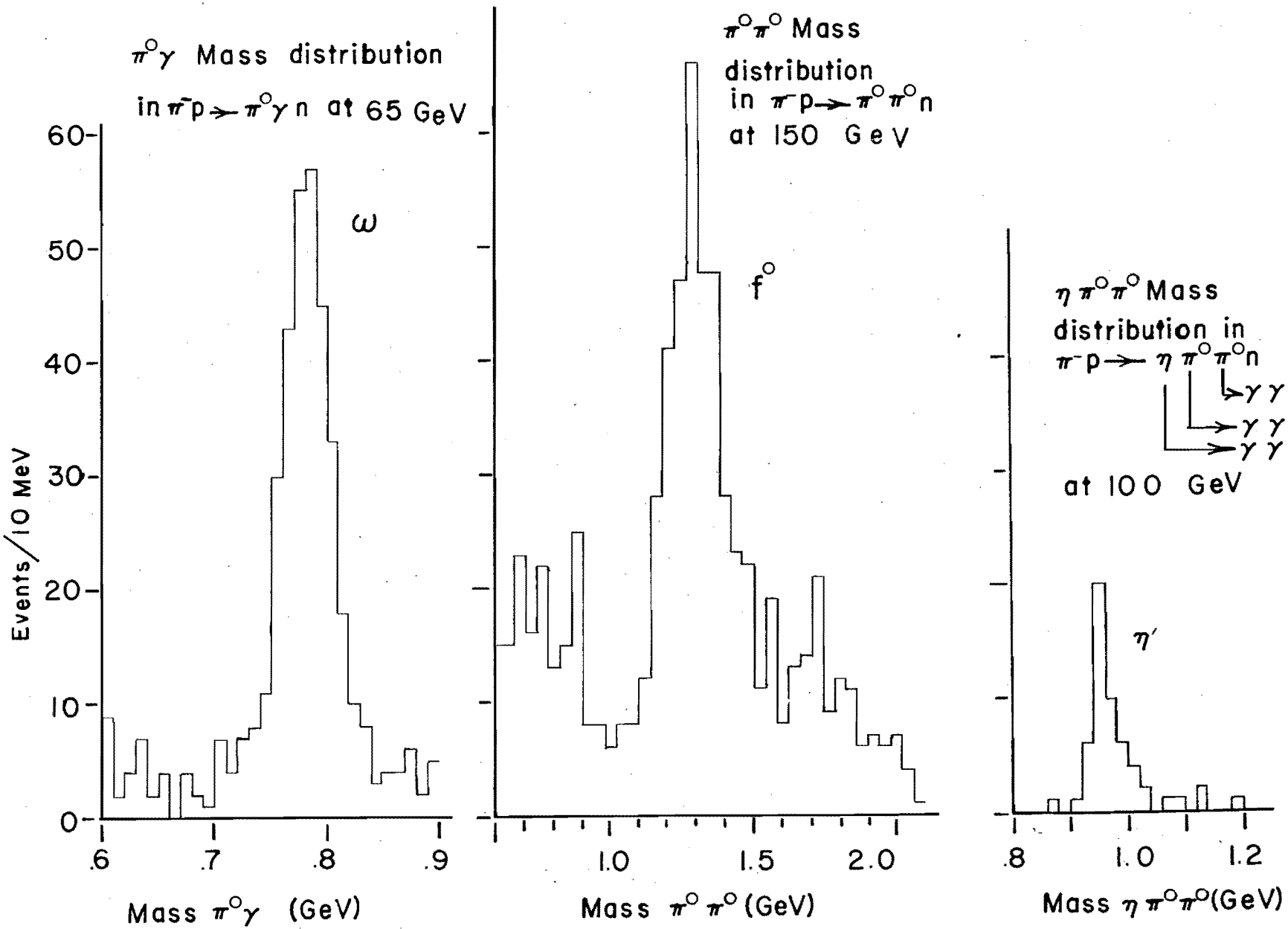
$\pi^0\gamma$ Mass distribution
in $\pi^- p \to \pi^0 \gamma n$ at 65 GeV
ω
Events/10 MeV
0
10
20
30
40
50
60
.6
.7
.8
.9
Mass $\pi^0\gamma$ (GeV)
$\pi^0\pi^0$ Mass
distribution
in $\pi^- p \to \pi^0 \pi^0 n$
at 150 GeV
f^0
1.0
1.5
2.0
Mass $\pi^0 \pi^0$ (GeV)
$\eta\pi^0\pi^0$ Mass
distribution in
$\pi^- p \to \eta \pi^0 \pi^0 n$
$\gamma\gamma$
$\gamma\gamma$
$\gamma\gamma$
at 100 GeV
η'
.8
1.0
1.2
Mass $\eta\pi^0\pi^0$(GeV)

FIGURE 5

IV. Acceptance, Resolution, and Yield Calculations

A. Reactions Yielding $\pi^+\pi^-\pi^o$ Forward in the Final State

The spectrometer as modeled for acceptance calculations is defined in Table V. Two positions were considered for the photon-detector. In position I the photon-detector is placed behind C_1. In position II the detector is placed behind C_2. The multiple scattering coefficients were obtained from members of Experiment #260 and the resolution of the gamma ray detector from Experiment #111.

The trigger for this experiment would be a requirement of two charged particles through the magnet and an energy requirement in the photon detector. Since the Cerenkov counters will enable us to distinguish between π's and K's, this trigger will include data on $\pi^+\pi^-\pi^o$, $\pi^+\pi^-\eta^o$, $K^\pm\pi^\mp\pi^o$, $K^+K^-\pi^o$ combinations. The analysis programs for the photon detector enable us to distinguish more than two photons; for example, $f^o \to \pi^o\pi^o \to 4\gamma$. The $(\pi^+\pi^-\pi^o)$ system has resonances at the η(mass = .549 GeV), ω(mass = .783 GeV), ϕ(mass = 1.020 GeV), A_2(mass = 1310 GeV), ω(mass = 1667 GeV), etc. Consequently, we looked at 3 different masses: .78 GeV, 1.2 GeV, and 1.6 GeV. The decays were assumed to be isotropic and the differential cross section from the E111 $\pi^-p \to \omega(\to\pi^o\gamma)n$ preliminary results were used. The shape of the differential cross section for higher mass particles was assumed to be the same as for the omega.

The resulting mass resolution is shown in Table VI. It is seen to be perfectly satisfactory to detect a narrow resonance. To study the acceptance a cut was applied which required that in at least one of the

Table V

Element	Distance from target (meters)	Width (meters)	Height (meters)	Multiple Scattering Coefficient	x Resolution (mm)	y Resolution (mm)	Other Properties
Target	0.			.036			.3 meters long, centered on 0 and of radius .01 meter
Proportional Chambers A	.71	.24	.24	.01	.2	.2	
Proportional Chambers B'	2.93	.72		.0025	.75		no y chamber
Proportional Chambers B	3.25	.84	.36	.005	.75	.75	
Proportional Chambers C	3.83	1.0	.60	.005	.75	.75	
Magnet	4.21						18 kilogauss, 1.02 meter long pole piece
Y-Aperture of Magnet	5.23		.60				
X-Aperture of Magnet	5.99	1.32					
Spark Chambers E	7.05	2.60	1.36		.3	.5	Includes D proportional chamber
Cherenkov Counter C1	12.25			.016			Only multiple scattering from mirrors at downstream end considered
Spark Chambers F	12.50	3.86	1.92		.3	.5	
Gamma Ray Detector	I:13.50 II:24.50	.735	.735				Energy resolution of $\pi^0 = .18/\sqrt{E(\mathrm{GeV})}$ Position resolution of $\pi^0 = .43$ mm.

Table VI: Mass Resolution for $\pi^{\pm}p \rightarrow (\pi^{+}\pi^{-}\pi^{o})X^{\pm}$

Incident Momentum	$\pi^{+}\pi^{-}\pi^{o}$ Effective Mass (GeV)		
	0.77GeV(ω^{o} mass)	1.2 GeV	1.6 GeV
40	11 MeV	17 MeV	19 MeV
100[a]	8 MeV	14 MeV	18 MeV
100[b]	8 MeV	12 MeV	16 MeV
200	11 MeV	16 MeV	20 MeV

(a) Photon detector located 13.5 m from target.

(b) Photon detector located 24.5 m from target.

two views (x and y planes) of the gamma ray detector the nearest charged particle was no closer than 10 cm to the center of the π^o. This cut is clearly only relevant at the higher energies where the charged particles are bent less by the magnet. It was also required that the center of the π^o be no closer than 3 cm to the edge of the detector. The resulting acceptances are shown in Table VII. From the E111 results we obtain a total ω^o cross-section of 3.5 μb at 40 GeV, 1 μb at 100 GeV, and .3μb at 200 GeV. Allowing for the branching ratio of 0.9 and for a cos θ cut on the π^o decay at 0.8 we estimate that in 100 hours one can see 45,000 omegas at 40 GeV, 12,000 omegas in position I at 100 GeV or 15,000 omegas in position II at 100 GeV, and 4,000 omegas in position II at 200 GeV. For the higher mass particles, it is harder to make estimates; thus at 6.95 GeV/c, Matthews et al.[9] find for $\pi^+\pi^-\pi^o$ decay:

$$\sigma(\pi^+ n \to \omega^o p) = 80\ \mu b$$

$$\sigma(\pi^+ n \to A_2^o p) = 54\ \mu b$$

$$\sigma(\pi^+ n \to \omega(1680) p) = 34\ \mu b.$$

Unfortunately Fox and Hey[10] claim you cannot scale these numbers to higher energy as the A_2^o and ω(1680) have a much larger B exchange contribution than ρ at low energies compared to the ω. Therefore as B exchange falls faster with energy than ρ, the high energy A_2 and ω(1680) cross-sections will be lower than the above ratios suggest. One may guess that our yield of these high mass resonances will be between 10 and 25% of the ω(783).

As mentioned above another decay observed simultaneously is the $\eta \to \pi^+\pi^-\pi^o$. The physics here is of lesser interest because the reaction $\pi^- p \to (\eta \to \gamma\gamma)n$ has been studied by E111 and because the η is spinless. The geometrical acceptance is high and its cross-section is similar to

Table VII Detection Efficiency for $\pi^{\pm}p \rightarrow (\pi^{+}\pi^{-}\pi^{o})X^{\pm}$

Incident Momentum	$\pi^{+}\pi^{-}\pi^{o}$ Effective Mass (GeV)		
	0.77 GeV (ω^{o} mass)	1.2 GeV	1.6 GeV
40 GeV[a]	0.75	0.34	0.12
100 GeV[a]	0.70	0.70	0.69
100 GeV[b]	0.91	0.64	0.46
200 GeV[b]	0.81	0.77	0.75

(a) Photon detector located 13.5 m from target.

(b) Photon detector located 24.5 m from target.

Assumptions:

1. Istropic distribution in the $\pi^{+}\pi^{-}\pi^{o}$ rest frame
2. Spatial separation at the detector between the π^{o} and charged $\pi \geq 10$ cm in at least one view.

that of the ω^o. However its branching ratio to $\pi^+\pi^-\pi^o$ will reduce its signal to about one-quarter of that of the omega.

Also, the η'(mass = .958 GeV) will be observed via its $\eta^o\pi^+\pi^-$ and $\rho^o\gamma$ decays and so over half the η''s produced should be observed. Our event yield for $\eta' \to \pi^+\pi^-(\eta,\gamma)$ is about a quarter of those quoted for the ω earlier.

B. Acceptance Studies for the Reaction $\pi^\pm p \to \Delta^+\pi^\pm$; $\Delta^+ \to p\pi^o$

The efficiency for detecting the p and π^o from the forward-going Δ^+ was determined by generating Monte Carlo events of the type:

$$\begin{array}{l} \pi p \to \Delta^+\pi \\ \quad\quad\;\; \hookrightarrow p\pi^o \\ \quad\quad\quad\quad \hookrightarrow \gamma\gamma \end{array} \qquad (9)$$

at incident beam momenta (p_{LAB}) of 20, 50, and 100 GeV/c. The Δ mass was chosen to be 1.236 GeV with a width of 0.1 GeV. In the p_{LAB} = 50 GeV/c case we also studied events with M_Δ = 1.700 GeV. We assumed an isotropic decay for the $\Delta \to p\pi^o$. In all cases, events were chosen such that u, the momentum-transfer squared between incoming π and outgoing Δ, follow a distribution of the form e^{Au} where A = 4.0 $(GeV/c)^{-2}$. The criteria satisfied by accepted events are:

a. the forward p go through the magnet

b. the two photons from the π^o enter the photon detector with both photons having an energy > 1.0 GeV.

c. the backward π^- is detected in the cylindrical PWC's.

Results of the Monte Carlo Studies

The kinematics of reaction (9) dictate certain features of the momentum spectra and angular distributions (with respect to the incoming beam direction) of the outgoing particles independent of the incident beam

momentum over the range of energies under discussion. The results below are for the Monte Carlo events integrated over the damped u distribution e^{Au}:

a. The protons from the Δ decay are well-collimated in momentum and direction as seen from the distributions in Figure 6. These indicate that essentially all the protons from reaction (9) will be detected and momentum-analyzed by the forward part of the spectrometer.

b. The backwards-going charged π is indeed emitted with $\theta > 90°$. The angular distribution is peaked at 135°. The momentum spectrum extends from ~0.5 and 1.5 GeV/c. It would be attractive to use the backward-going pion signature in the trigger. However, the current division readout used to determine positions in the cylindrical PWC's cannot be used in the trigger. The determination that the slow particle is emitted backwards will be a powerful constraint in the off-line analysis of the data.

c. The detection efficiencies for reaction (9) for various positions of the photon-detector are shown in Table VIII. These efficiencies, along with cross sections extrapolated from lower energy data, give rise to the expected yields listed in Table IX.

<u>$\pi p \rightarrow \Delta\pi$ Trigger and Background Triggers</u>

The trigger requirements for the forward Δ reaction are:

a. a single charged particle detected by the cylindrical proportional wire chambers (α and β) around the target;

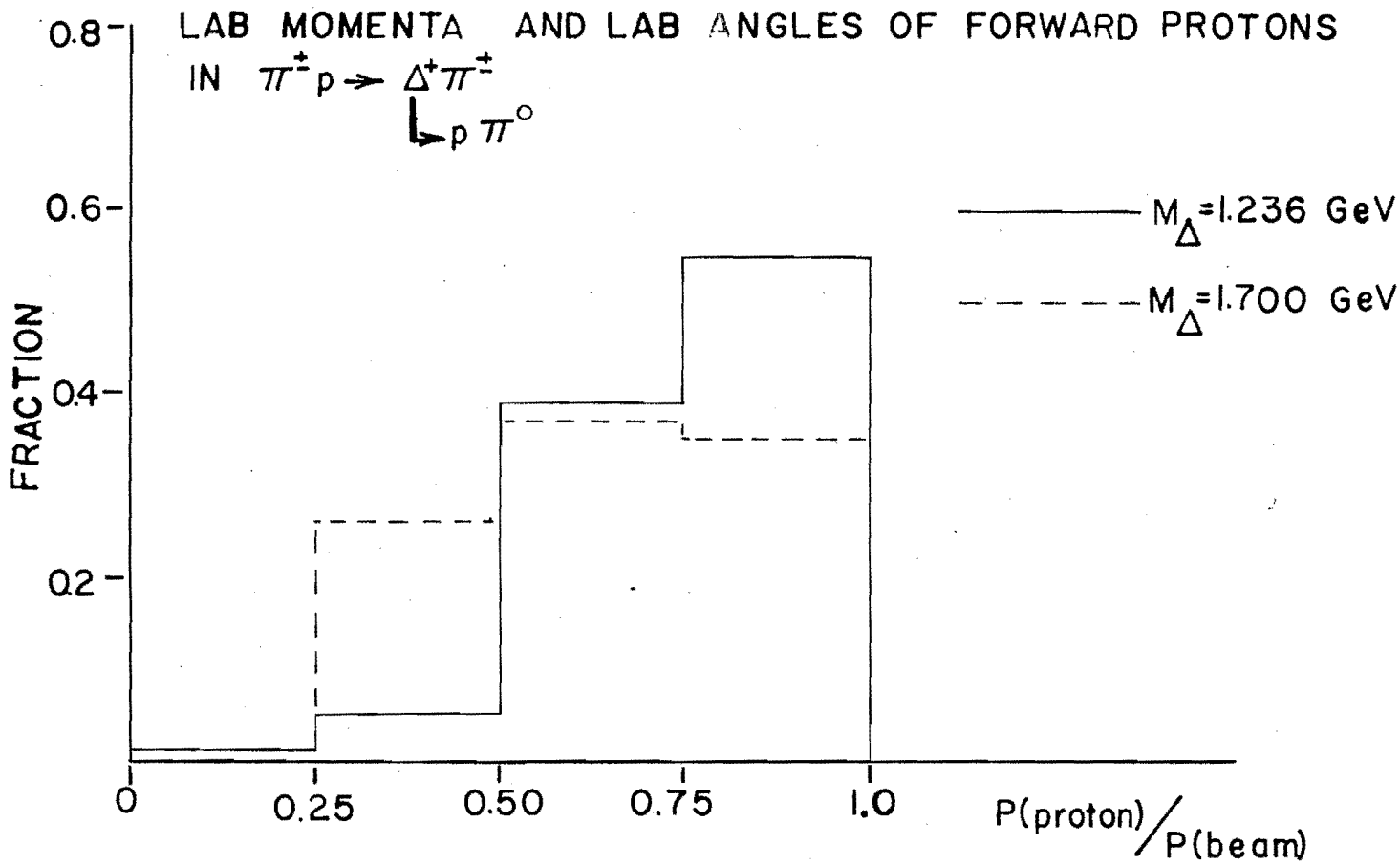
LAB MOMENTA AND LAB ANGLES OF FORWARD PROTONS
IN $\pi^{\pm} p \rightarrow \Delta^{+}\pi^{\pm}$
$\hookrightarrow p\,\pi^{0}$
M_{Δ}=1.236 GeV
M_{Δ}=1.700 GeV
FRACTION
0.8
0.6
0.4
0.2
0
0.25
0.50
0.75
1.0
P(proton)/P(beam)

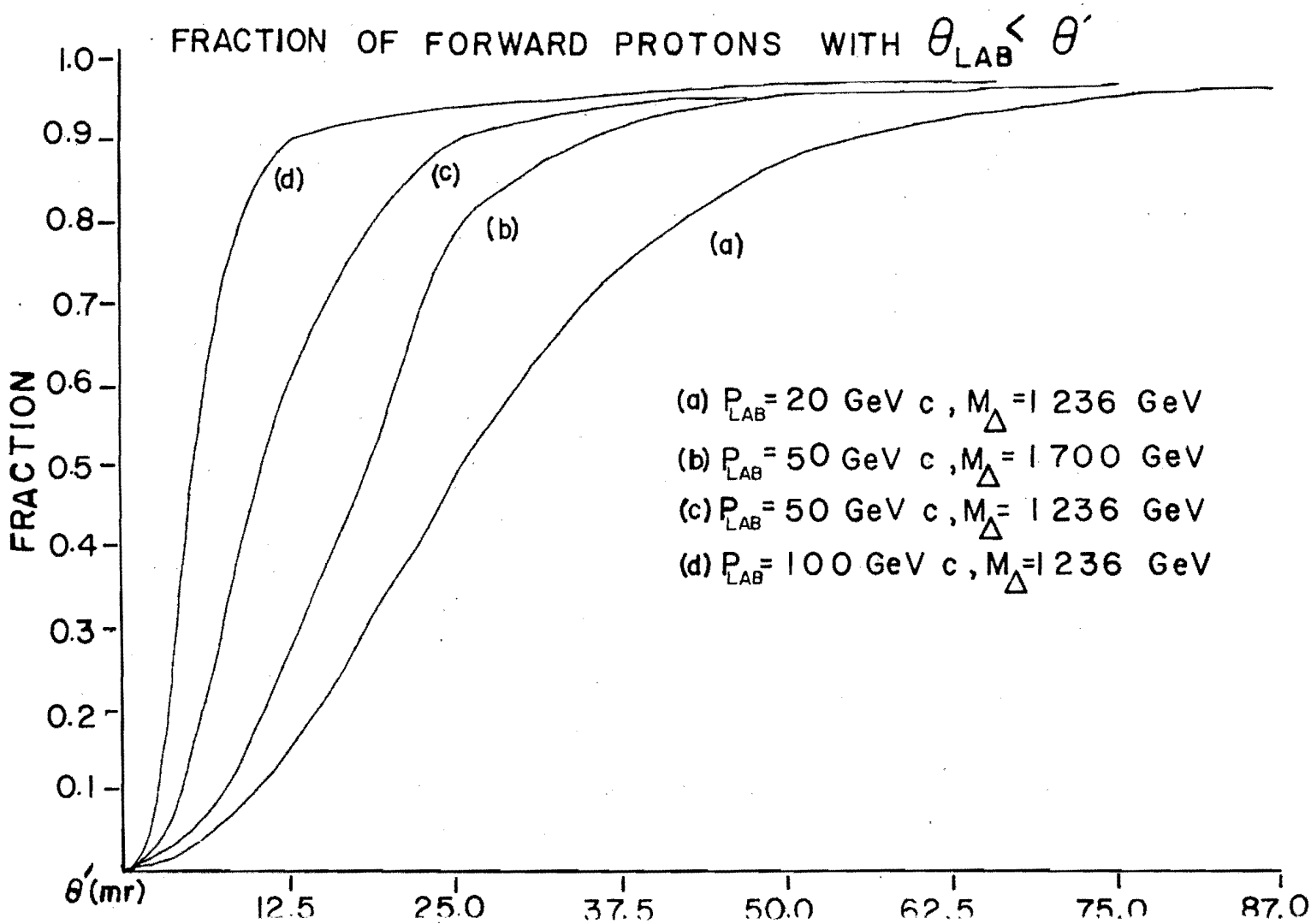
FRACTION OF FORWARD PROTONS WITH $\theta_{LAB} < \theta'$
FRACTION
1.0
0.9
0.8
0.7
0.6
0.5
0.4
0.3
0.2
0.1
(a)
(b)
(c)
(d)
(a) P_{LAB}= 20 GeV c , M_{Δ}=1 236 GeV
(b) P_{LAB}= 50 GeV c , M_{Δ}= 1 700 GeV
(c) P_{LAB}= 50 GeV c , M_{Δ}= 1 236 GeV
(d) P_{LAB}= 100 GeV c , M_{Δ}=1 236 GeV
θ'(mr)
12.5
25.0
37.5
50.0
62.5
75.0
87.0

Table IX: Yields for $\pi^{\pm}p \rightarrow \Delta^{+}\pi^{\pm}$

p_{LAB} (GeV/c)	Beam Charge	Photon Detector Z-Position (m)	Cross Section (μb)	Yield Events/ Burst	Hours of Run	Yield (Events)
20	+	7.5	.036	.036	100	1000
	−			.037	100	1300
50	+	13.5	.0058	.006	200	400
	−			.012	100	400
100	+	13.5	.0015	.002	150	100
	−			.006	200	400

These yields were calculated assuming:

a. Detection efficiencies in Table VIII

b. A u and energy dependence of the form (as parameterized by F. Hayot)

$$\frac{d\sigma}{du} = K\, p_{LAB}^{-n}\, A\, e^{Au}\, \frac{\mu b}{(GeV/c)^2}$$

$K = 58$
$n = 2$
$A = p_{LAB}$ in GeV/c
$u = (GeV/c)^2$

c. Safety factor of 0.25 for unknown dynamics and anticipated inefficiencies

d. FNAL rep rate of 10 sec and 5×10^6 beam particles/burst.

b. sufficient energy in the photon detector; and

c. a single charged particle forward which does not count in the Cerenkov counters C_1 and C_2.

The primary background triggers will arise from:

a. Pion-induced diffractive process such as

$$\pi^- p \rightarrow \pi^- \pi^o \pi^o p$$

which yield a forward π^- and π^o and a slow proton. The cross section for this process is large (100's of μb) and falls slowly with incident momentum. In fact, we expect forward π's to be produced 10^6 more copiously than protons.[12] Inefficiencies in the C_1 and C_2 Cerenkov counters will thus allow these reactions to contaminate our trigger.

The Cerenkov counters C_1 and C_2 are capable of detecting relativistic π's with an inefficiency of 10^{-5}. For example, assuming 50% optics efficiency at 50 GeV/c, C_1 and C_2 will have an average number of photoelectrons coming from 20 GeV/c pions of 18.5 and 37, respectively. Even allowing another factor of 50% photon loss (say from pions with off-axis trajectories), the C_1 and C_2 joint inefficiency is still much less than 10^{-6}. At 100 GeV/c the corresponding joint C_1C_2 inefficiency (for 50 GeV/c pions) climbs to 5×10^{-4}. Without the last 50% photon attenuation factor, the inefficiency would be 3×10^{-7}. To the extent that we depend on C_1 and C_2 having a 10^{-5} inefficiency, we see that at the highest energy the situation is somewhat precarious. We plan test runs to study the C_1 and C_2 efficiencies in detail. Thus, we expect that C_1 and C_2 alone (especially at the highest momenta) will not adequately suppress forward pion triggers.

To improve the trigger selection we plan to use the vertical wires upstream and downstream of the analyzing magnet (Stations B and F" in Figure 1) in the trigger. The charge of the forward particle will be easy to deduce using B and F". Thus, for $\pi^- p$ running forward π^-'s will be completely stifled in their attempt to simulate p's. Our Monte Carlo studies of $\pi^+ p \rightarrow (\pi^+\pi^o)_{fwd}(\pi^+ n)_{bkwd}$ show that only high-momentum π^o's satisfy the trigger; the forward π^+ then has ≤50% of the beam momentum and shows a B-F" hit pattern which is enough different from desired events that about 2/3 of these events can be eliminated using B and F.

b. Proton induced reactions such as

$$pp \rightarrow N^* p$$
$$\quad\quad \hookrightarrow p\pi^o$$

will contaminate our trigger when we run with the positive beam, which has an admixture of protons. At 20 GeV/c, the π^+/p ratio is about 3½ to 1; at 100 GeV/c, the π^+/p ratio is 1 to 2. Since forward protons are produced about 10^6 more readily with protons than with pions, we need a beam Cerenkov system capable of identifying protons with an inefficiency of 10^{-7} or less. We plan to use the two threshold beam Cerenkovs in coincidence and expect them each to give false proton signals (from knock-on electrons) less than 1% of the time. The differential Cerenkov counters will be set to detect protons with an efficiency exceeding 99%. The joint rejection of protons is then 10^8. Although these Cerenkov requirements are within their design capabilities, we plan to measure them during a test run.

If a proton and pion share the same beam rf bucket, the threshold counters are not of value. We will avoid this situation (at the 99% level) by doing pulse height analysis on the beam particles and eliminating rf buckets with >1 charged particle. There will be a downstream counter requiring the beam to interact. Since only about 10% of the beam interacts, we gain another factor of 10 suppression of these shared-bucket events.

Conclusion

We expect our trigger rate from non-pathological reactions to be comparable to our desired trigger rate. Since we can easily handle 10 triggers/burst, the trigger seems suitably exclusive - except perhaps at the highest beam momentum as discussed above.

Summary

We plan to emphasize running with negative particles at the outset of the experiment. Then we can avoid dealing with the proton admixture in the beam. Also, the forward meson reactions have a simpler trigger with π^- than with π^+ beams because the recoil baryon system has charge zero. Finally, the baryon exchange studies have a much cleaner trigger with π^-'s because the forward proton charge is different from the background of beam-diffracted systems.

We will be ready to begin this experiment in late Spring, 1977 --right after the completion of E110. Except for some minor supplements (as discussed in the proposal) all hardware exists and has been exhaustively debugged while Experiments E260 and E111 were executed by us (and other collaborators). Our software is similarly in a proven state.

References

1. A. Barnes et al., Phys. Rev. Letters 37, 76 (1976).
2. A. Dzierba et al., Fermilab Proposal 110, and G. Fox et al., Fermilab Proposal 110 Amended 5-5-74.
3. G. Fox et al., Fermilab Proposal 260.
4. O. I. Dahl et al., Phys. Rev. Letters 37, 80 (1976).
5. Holloway et al., Phys. Rev. D8, 2814 (1973).
6. T. Inami et al., Univ. of Tokyo preprint, UT-Konaba 76-1.
7. The reader is referred to an excellent review by G. C. Fox: "Peripheral Production of Resonances" in A.I.P. Conference Proceedings No. 8, Particle and Fields Subseries No. 3 Experimental Meson Spectroscopy - 1972, edited by A. Rosenfeld and K.-W. Lai. The reader is however warned not to be too enraptured by the poetic and literary impact of this work. (A.R.D.). See also Reference 10.
8. Additional details regarding the photon detector contained in several Caltech Internal Reports and in the thesis of R. A. Johnson (LBL Report LBL-4610).
9. Matthews et al., Phys. Rev. D3, 2561 (1971).
10. Fox and Hey, Nucl. Phys. B56, 386 (1973).
11. Babaev et al., Phys. Letters 38B, 342 (1972).
12. Anderson et al., Phys. Rev. Letters 37, 1111 (1976).